

Temperature dependence of the magnetic volume susceptibility of human breast fat tissue: an NMR study

Sara M. Sprinkhuizen · Chris J. G. Bakker ·
Johannes H. Ippel · Rolf Boelens · Max A. Viergever ·
Lambertus W. Bartels

Received: 22 November 2010 / Revised: 25 February 2011 / Accepted: 28 March 2011 / Published online: 12 April 2011
© The Author(s) 2011. This article is published with open access at Springerlink.com

Abstract

Object Proton resonance frequency shift (PRFS)-based MR thermometry (MRT) is hampered by heat-induced susceptibility changes when applied in tissues containing fat, e.g., the human breast. In order to assess the impact of fat susceptibility changes on PRFS-based MRT during thermal therapy in the human breast, reliable knowledge of the temperature dependence of the magnetic volume susceptibility of fat, $d\chi_{\text{fat}}/dT$, is a prerequisite. In this work we have measured $d\chi_{\text{fat}}/dT$ of human breast fat tissue, using a double-reference method to ensure invariance to temperature-induced changes in the proton electron screening constant.

Materials and methods Ex vivo measurements were taken on a 14.1 T five mm narrow bore NMR spectrometer. Breast fat tissue samples were collected from six subjects, directly postmortem. The susceptibility was measured over a temperature range from 24°C to 65°C.

Results A linear behavior of the susceptibility over temperature was observed for all samples. The resulting $d\chi_{\text{fat}}/dT$ of human breast fat ranged between 0.0039 and 0.0076 ppm/°C.

Conclusion It is concluded that the impact of heat-induced susceptibility changes of fat during thermal therapy in the breast may not be neglected.

Keywords Magnetic volume susceptibility · NMR spectroscopy · Breast · Fat · Temperature · Temperature dependence · Thermometry

Introduction

The increasing interest in MRI-guided thermal ablation therapy for breast tumors has heightened the need for reliable MR thermometry (MRT) techniques in tissues with high fat content. The currently most widely used MRT technique is proton resonance frequency shift (PRFS)-based MRT, which exploits the temperature dependence of the electron screening constant of water ($d\sigma_{\text{water}}/dT = 0.01\text{ppm}/^\circ\text{C}$ [1]). The electron screening constant of fat is near-independent of temperature [2], and fat suppression techniques are therefore employed for PRFS-based MRT in fat-containing tissues. The contribution of changes in the magnetic volume susceptibility χ (which will hereinafter be referred to as ‘susceptibility’) to the water proton resonance frequency (PRF) is commonly ignored in PRFS-based MRT. This disregards the fact that the susceptibility of fat, χ_{fat} , is temperature dependent [2, 3]. Heating-induced changes in the susceptibility distribution lead to non-local magnetic field changes. This, in turn, affects the PRF and, hence, the measured temperature of all water protons that experience this magnetic field change. Heating-induced susceptibility changes may therefore lead to errors in PRFS-based MR thermometry measurements during thermal therapy in tissues with high fat content, even when fat suppression techniques are employed. This has previously been shown for breast tumor ablation using High Intensity Focused Ultrasound (HIFU) [4].

In order to be able to estimate the impact of heating-induced susceptibility changes of fat on PRFS-based MRT during thermal therapy in the human breast, accurate

S. M. Sprinkhuizen (✉) · C. J. G. Bakker · M. A. Viergever ·
L. W. Bartels

Image Sciences Institute/Department of Radiology, University
Medical Center Utrecht, Room Q0S.459, Heidelberglaan 100,
3584 CX, Utrecht, The Netherlands
e-mail: sara.sprinkhuizen@gmail.com

J. H. Ippel · R. Boelens
NMR Spectroscopy Research Group, Bijvoet Center
for Biomolecular Research, Utrecht University, Padualaan 8,
3584 CH, Utrecht, The Netherlands

measurements of the temperature dependence of the susceptibility, $d\chi/dT$, of human breast fat tissue are a prerequisite. However, values of the temperature dependence of the susceptibility of fat found in the literature were based on in vitro experiments in porcine fat samples, one of which was pre-cooked fat [2,3]. In two in vivo studies, cooling of human calf tissue did not reveal temperature dependence of the susceptibility of fat, but these studies were performed at 1 T and 1.5 T and covered only small temperature ranges [5,6].

In this work we aimed to measure $d\chi/dT$ of human breast fat tissue. Since we are interested in susceptibility effects during thermal ablation therapy of breast tumors, the measurements were taken over a large temperature range (42 degrees Celsius). A technique from the field of NMR spectroscopy was applied, the double-reference method [7], which was developed to measure susceptibility while being invariant to the temperature dependence of the proton electron screening constant. This approach allows for derivation of susceptibility values from a single spectrum and therefore allows for $d\chi/dT$ measurements within one heating–cooling cycle. The experiments were performed on a 14.1 T NMR spectrometer for increased accuracy and precision.

Materials and methods

NMR spectroscopy

High-resolution NMR spectra were acquired on a Bruker Avance Ultrashield spectrometer (Bruker Biospin GmbH, Rheinstetten, Germany) operating at a ^1H frequency of 600 MHz and equipped with a triple resonance 5 mm TXI probe. A standard Bruker BVT-1000 variable temperature unit (VTU) was used to regulate the temperature of the air stream directed into the NMR probe. Temperature calibration was made prior to the experiments to eliminate differences between the temperature as indicated on the spectrometer, T_{spectro} (which is that of the thermocouple mounted near the sample), and the true sample temperature, T_{sample} . This was done by using a dedicated temperature calibration sample (Bruker, 80% glycol/20% DMSO- d_6) for a range of T_{spectro} temperatures, starting at $T_{\text{spectro}} = 24.85^\circ\text{C}$ (298 K) up to $T_{\text{spectro}} = 54.85^\circ\text{C}$ (328 K), in steps of 1°C . To ensure sufficient time for homogeneous temperature distribution within the sample, a temperature equilibration period of 20 min was allowed after the sample temperature had reached each step in the temperature sequence. Per spectrum, 4 scans were accumulated. The acquisition time was 0.85 s, the spectral width was 16 ppm, and the interscan delay was set to 5 s to ensure complete recovery of equilibrium magnetization. Per spectrum, the actual temperature of the calibration sample was calculated using the empirically derived relationship

(Bruker VTU manual):

$$T_{\text{sample}}(^{\circ}\text{C}) = \frac{4.218 - \Delta}{0.009132} - 273.15 \quad (1)$$

where Δ is the chemical shift difference in ppm between the proton signals of the OH group and CH_2 group of glycol. For all fat susceptibility measurement experiments, the same heating protocol was applied, and the temperature as indicated on the spectrometer was converted to the calibrated sample temperature.

Fat tissue samples

Breast fat tissue samples were collected from six subjects directly postmortem (all voluntary whole body donation, age subject I: 75, II: 50, III: 80, IV: 69, V: 93, VI: 78 years). The tissue samples were transferred into a 5-mm NMR sample tube. Air bubbles are detrimental for accurate susceptibility measurements and were removed as much as possible in the final NMR samples. Since our aim was to measure susceptibility changes of the tissue, no reference solvent or conservatives (e.g., formaldehyde) were added to the samples.

Measurement of $d\chi/dT$

To measure the temperature dependence of the susceptibility of fat tissue, without being hampered by changes in its proton electron screening constant σ , NMR experiments were performed using a double-reference method [7]. This method employs a capillary-sphere (*cs*)-insert, filled with a reference solvent, which is placed inside a thin-walled NMR sample tube containing the fat tissue (Fig. 1, Wilmad (Buena, NJ, USA; catalog item 529-A)).

The magnetic field experienced by the nuclei of the reference solvent, B_{nuc} , is related to the location of the nuclei within the *cs*-insert. This is shown by Eqs. 2 and 3, which describe the magnetic field at the nucleus inside a perfect cylinder, parallel to the main magnetic field, and sphere:

$$B_{\text{nuc, capillary}} = B_0 \left(1 - \sigma_{\text{ref}} + \frac{\chi_{\text{ref}}}{3} \right) \quad (2)$$

$$B_{\text{nuc, sphere}} = B_0 \left(1 - \sigma_{\text{ref}} + \frac{\chi_{\text{sample}}}{3} \right) \quad (3)$$

with B_0 the main magnetic field, σ_{ref} the proton electron screening constant of the reference solvent, χ_{ref} the susceptibility of the reference solvent, and χ_{sample} the susceptibility of the sample. In the spectrum of the *cs*-setup, two separate reference solvent peaks appear. The chemical shift difference in the positions $\delta_{\text{ref, capillary}}$ and $\delta_{\text{ref, sphere}}$ of the two reference solvent peaks is related to the difference in susceptibility between the reference solvent and the fat sample surrounding the reference solvent:

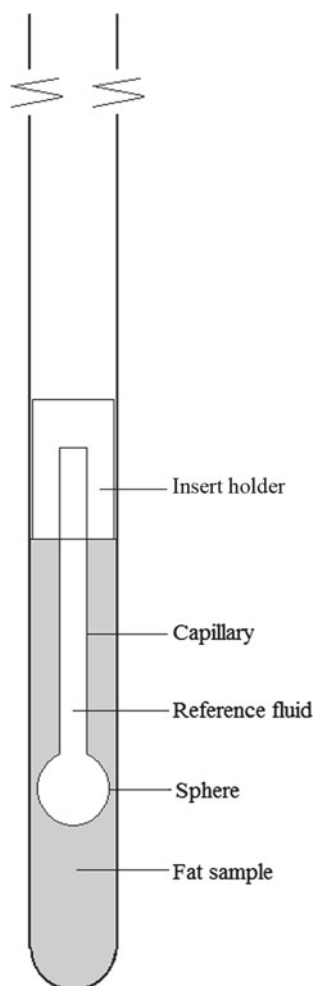


Fig. 1 The experimental setup, consisting of a capillary-sphere (*cs*) insert, filled with reference fluid, which is placed inside a 5-mm NMR sample tube. The sphere of the *cs*-insert was located in the center of the receiver coils sensitivity (positioned around 2.5–3 cm upwards as seen from the bottom of the NMR tube). The length of the *cs*-insert was 45 mm, the filling of the sample was ensured to be up to the height of the insert holder

$$\delta_{\text{ref, capillary}} - \delta_{\text{ref, sphere}} = (g_{\text{capillary}} - g_{\text{sphere}}) \times (\chi_{\text{ref}} - \chi_{\text{sample}}) \quad (4)$$

in which $(g_{\text{capillary}} - g_{\text{sphere}})$ is a factor related to the geometry of the setup, which will be referred to in more detail below. Subsequently, χ_{sample} can be calculated using Eq. 5:

$$\chi_{\text{sample}}(T) = \chi_{\text{ref}}(T) - \frac{\delta_{\text{capillary}} - \delta_{\text{sphere}}}{G} \quad (5)$$

Theoretically, the geometry factor $G = (g_{\text{capillary}} - g_{\text{sphere}}) = 1/3$ for a setup with a separate, perfect sphere and parallel cylinder. The shape of the *cs*-insert, however, is not a perfect cylinder and sphere, as shown in Fig. 1. G therefore needs to be predetermined by a calibration experiment, using a

reference fluid and sample fluid with known susceptibilities:

$$G = \frac{\delta_{\text{ref, capillary}}[\text{ppm}] - \delta_{\text{ref, sphere}}[\text{ppm}]}{(\chi_{\text{ref}} - \chi_{\text{sample, Gcal}})} \quad (6)$$

The susceptibility of the sample fluid used for the G -calibration experiment is referred to as $\chi_{\text{sample, Gcal}}$, to avoid confusion with the susceptibility of the sample of interest.

In our application, the reference fluid in the *cs*-insert had to fulfill three requirements. First, its resonance peaks needed to lie well outside the fat tissue spectra covering 0.5–6 ppm. Furthermore, its signal intensity had to be sufficiently high to accurately determine the chemical shift difference of the two separate solvent peaks in the *cs*-insert. And last, its susceptibility had to have a known temperature dependence. Chloroform (CHCl_3) was chosen for our application. Although the temperature dependence of the susceptibility of CHCl_3 has not been reported in literature, it has been reported for the deuterated variant (CDCl_3). As is stated by Hoffman et al. [8], the temperature dependence of the susceptibility of CHCl_3 equals that of CDCl_3 , since it is reasonable to assume that isotopic substitution does not significantly affect the density variation with temperature and that the molar susceptibility is temperature independent. We thus used the following equation for the temperature dependence of CHCl_3 (based on Eq. 8 from [8]):

$$\chi_{\text{CHCl}_3}(\text{ppm}) = 4\pi(1.18 \times 10^{-11}T^4 + 8.8 \times 10^{-10}T^3 + 2.57 \times 10^{-7}T^2 + 9.27 \times 10^{-4}T - 0.7556) \quad (7)$$

where T is the temperature in $^{\circ}\text{C}$.

In this work, the temperature dependence of the magnetic susceptibility of fat tissue samples is measured using a technique that was previously developed for susceptibility measurements at constant temperatures. Our interest in measurements over a range of temperature range thus required an extra procedure, being the determination of setup related geometry factor G over the same temperature range. The calibration of the geometry factor G was made with CHCl_3 in the *cs*-insert and deuterated dimethyl sulfoxide (DMSO-d^6) as the sample solvent in the NMR tube. The temperature dependence of the susceptibility of DMSO-d^6 was reported by Hoffman et al. (based on Eq. 9 from [8]):

$$\chi_{\text{DMSO-d}^6}(\text{ppm}) = 4\pi(3.30 \times 10^{-7}T^2 + 5.13 \times 10^{-4}T - 0.6245) \quad (8)$$

where T is the temperature in $^{\circ}\text{C}$. To determine the geometry factor G for our *cs*-sphere setup, eight 1D spectra were acquired at temperatures between $T = 23.5^{\circ}\text{C}$ and $T = 63^{\circ}\text{C}$. For the recording of the geometry calibration spectra, long equilibration times were employed (15 min) between successive temperature points. Per spectrum, 4 scans were accumulated. The interscan delay was set to 5 s, the acquisition time was 0.85 s, and the spectral width was 16 ppm.

The CHCl_3 -filled *cs*-insert, which was used for the geometry calibration experiment, was cleaned with ethanol and transferred into the fat tissue sample tube. The capillary-sphere insert with a length of 45 mm was positioned in the NMR tube with the spherical part located in the center of the receiver coil, 2.5–3 cm in the *z*-axis direction. It was ensured that the fat sample filled the NMR tube covering the complete length of the insert, therefore covering typically 7 cm from the bottom of the NMR tube.

Series of 1D proton spectra of the *cs*-setup were acquired covering a temperature interval between $T = 23.5^\circ\text{C}$ and $T = 65.4^\circ\text{C}$. Both the upward and downward temperature profiles (31 temperature points each) were acquired to investigate possible hysteresis effects due to temperature-induced changes in the fat tissue sample. To ensure a homogeneous temperature distribution within the sample, a temperature equilibration period of 20 min was used at every temperature point. Typically, 16 scans were accumulated per spectrum. The acquisition time was 0.85, the spectral width was 16 ppm, and the interscan delay was set to 5 s to ensure complete recovery of equilibrium magnetization. Prior to and after the complete heating–cooling cycle, the sample was visually inspected to detect possible changes in the fat tissue.

NMR spectra were collected in the absence of a deuterated solvent in the fat tissue or the *cs*-insert and thus without the possibility of field lock. The short-term and long-term field drift of the ultrashielded magnet in unlocked mode amounts to less than 2 Hz per day and therefore the magnetic field stability was considered sufficiently good to repeatedly extract the absolute chemical shift changes over time during the temperature series of the fat samples. Proton chemical shifts were given with reference to tetramethylsilane (TMS) that was dissolved in the chloroform of the *cs*-insert. The most upfield shifted line of TMS arising from the capillary part was used as the 0 ppm reference.

Data analysis

All spectra were acquired with Bruker Topspin 2.1 software and analyzed using MestRe-C 4.9.9.6 [Mestrelab Research, Santiago de Compostela, Spain]. The acquired FID's were apodized with a 10-Hz exponential filter prior to the Fourier transform. Zeroth- and first-order phase corrections were manually applied per spectrum to achieve a flat baseline over the entire spectral range. The peak positions $\delta_{\text{capillary}}$ and δ_{sphere} of the reference solvent were then determined by the peak picking algorithm as implemented in MestRe-C. The susceptibility of the fat tissue was calculated per spectrum (i.e., per temperature step) using Eqs. 5 and 7 and was plotted against temperature. A linear fit was made to determine $d\chi_{\text{fat}}/dT$ for each sample and the goodness of fit was evaluated using the coefficient of determination (R^2).

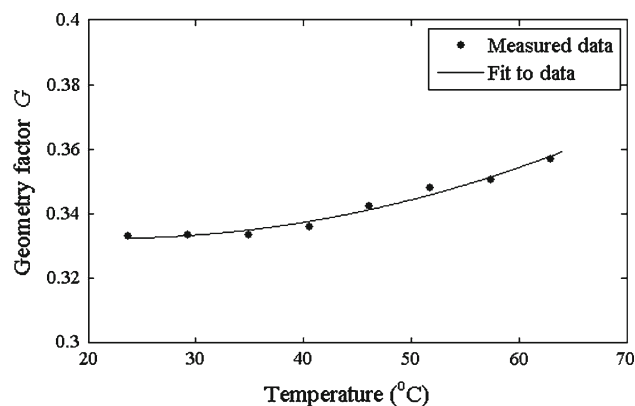


Fig. 2 Outcome of the calibration of the geometry factor G , showing the temperature dependence of G . Both the experimental outcome and the second-order polynomial fit are shown

Table 1 The assigned peaks from the triacylglyceride spectrum of the human breast fat

Peak nr.	Chemical group
1	–CH=CH–
2	H₂O
3	–CH₂–O–C(O)–CH₂–CH₂–
4	–CH₂–O–C(O)–CH₂–CH₂–
5	–CH=CH–CH₂–CH=CH–
6	–CH₂–O–C(O)–CH₂–CH₂–
7	–CH₂–CH=CH–CH₂
8	–CH₂–O–C(O)–CH₂–CH₂–
9	–(CH₂)_n–
10	CH₃–(CH₂)_n–

The corresponding protons in the spectra are indicated with a bold font

Results

The geometry factor calibration results are shown in Fig. 2. A temperature dependence of the geometry factor was observed. A second-order polynomial was fitted to the outcome of the G -calibration using a nonlinear least squares trust region fit procedure (Mathworks, Natick, MA, USA). The result of the fitting procedure was as follows: $G(T) = aT + bT^2 + c$ with the following coefficients (and 95% confidence bounds): $a = -6.58 \times 10^{-4} (-1.55 \times 10^{-3}, 2.37 \times 10^{-4})$; $b = 1.51 \times 10^{-5} (4.80 \times 10^{-6}, 2.53 \times 10^{-5})$; $c = 0.3397 (0.321, 0.358)$. This fit result was used to interpolate the outcome of the G -calibration data to all temperature values within the heating–cooling cycle (gray line).

Two 1D spectra of human breast fat, acquired at two different temperatures ($T = 23.52^\circ\text{C}$ and at $T = 65.43^\circ\text{C}$), are shown in Fig. 3. The assigned peaks from the triacylglyceride spectrum of the human breast fat are listed in Table 1 [9]. A part of the spectrum zoomed at the location of the CHCl_3 reference peaks ($\delta_{\text{ref, capillary}}$, right peak and $\delta_{\text{ref, sphere}}$, left peak) is shown.

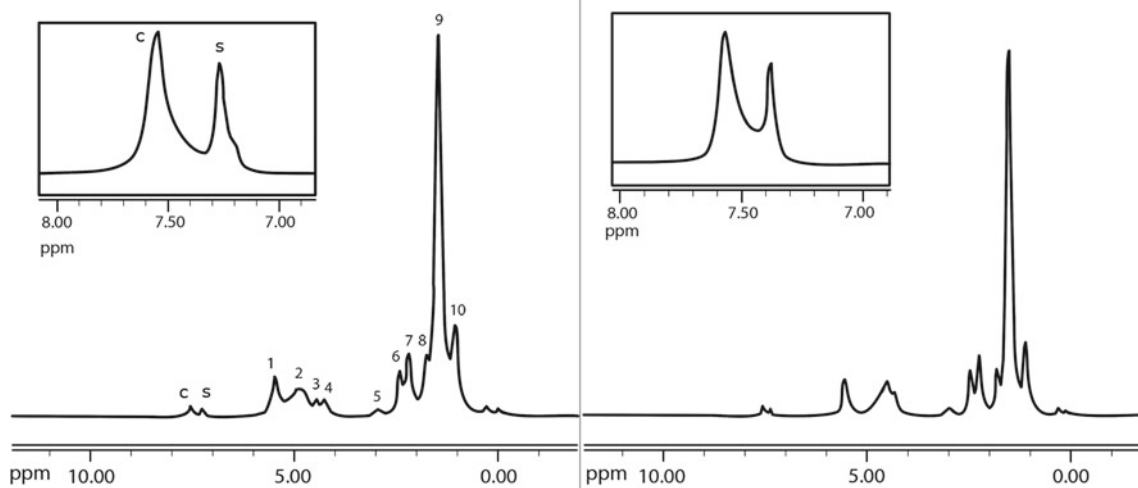


Fig. 3 Two spectra of breast fat tissue (sample VI), at $T = 23.5^{\circ}\text{C}$ (left) and at $T = 65.4^{\circ}\text{C}$ (right). On the far left, the two CHCl_3 reference peaks are visible. A zoomed version of both spectra at the location of the two reference peaks (capillary peak (left) and sphere peak

(right)) is shown in the inset. The frequency difference between the two peaks was 0.28 ppm at $T = 23.5^{\circ}\text{C}$ ($G = 0.333$) and 0.19 ppm at $T = 65.4^{\circ}\text{C}$ ($G = 0.361$)

The measured susceptibility of breast fat over temperature for all six samples is shown in Fig. 4. The measurements of the whole heating–cooling cycle are plotted. For all samples, a temperature dependence of the magnetic volume susceptibility is observed. The results of a linear fit through the data are presented in Table 2. The corresponding R^2 values show that the linear fit represents the behavior of the susceptibility over temperature up to a high level of accuracy. The average $d\chi_{\text{fat}}/dT$ and its standard deviation over all samples was $0.0048 \pm 0.0007 \text{ ppm}/^{\circ}\text{C}$ during slow heating and $0.0061 \pm 0.0012 \text{ ppm}/^{\circ}\text{C}$ during slow cooling.

There is a spread in the absolute χ values of the samples of $\sim 0.5 \times 10^{-6}$. The values are, however, in agreement with the reported susceptibility value of animal fat (-7.79×10^{-6}) [10].

All fat tissue samples were opaque prior to the measurement of $d\chi_{\text{fat}}/dT$. After the experiments, four out of the six fat tissue samples (I, II, III, and IV) had become partially translucent. The composition of these samples was altered during the heating, and an oily substance was present, likely due to redistribution of emulsified or fatty acid components in the sample. However, in two cases (V and VI), the samples were still opaque after the heating–cooling cycle.

Discussion

The measured $d\chi_{\text{fat}}/dT$ values ranged from 0.0039 up to 0.0076 $\text{ppm}/^{\circ}\text{C}$ between the samples. These values are somewhat smaller, but in the same order of magnitude as the reported temperature dependence of χ_{fat} in porcine pre-cooked fat ($0.00804 \pm 0.00145 \text{ ppm}/^{\circ}\text{C}$ [2]). The spread in $d\chi_{\text{fat}}/dT$ may be explained by intersubject variation in

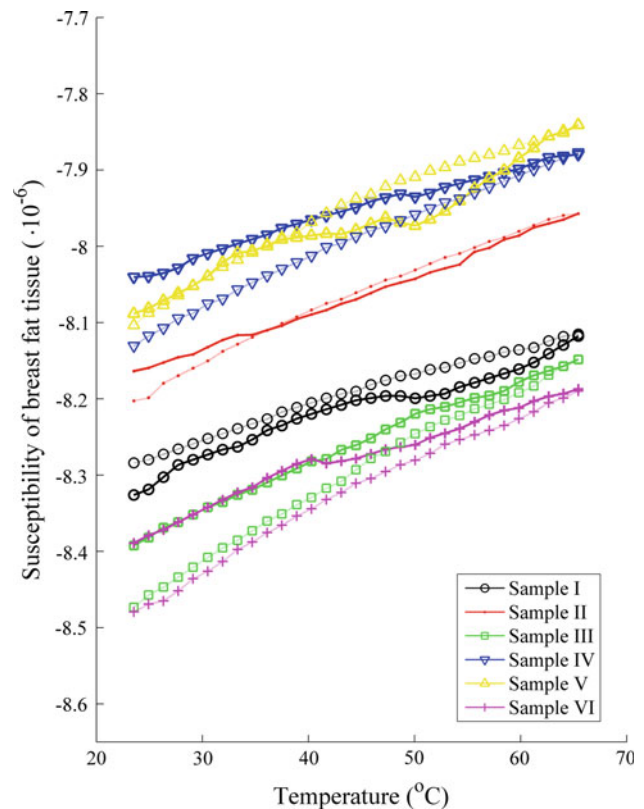


Fig. 4 The temperature dependence of the magnetic susceptibility χ_{fat} of six different human breast fat samples. The results acquired during the heating period are indicated by thicker solid lines, the results during the cooling are shown by thin dotted lines

fat composition, or the presence of blood traces in the fat (addressed in more detail below). Redistribution of the lipid material after de-emulsifying the fatty matrix at elevated

Table 2 Temperature dependence of the susceptibility of six breast fat samples during temperature rise (second column) and temperature fall (fourth column)

Sample	$d\chi_{\text{fat}}/dT$ (ppm/°C) Temperature rise	R^2	$d\chi_{\text{fat}}/dT$ (ppm/°C) Temperature fall	R^2
I	0.0042	0.96	0.0041	0.99
II	0.0050	0.99	0.0059	0.99
III	0.0057	0.99	0.0076	0.99
IV	0.0039	0.99	0.0059	0.99
V	0.0052	0.95	0.0061	0.98
VI	0.0045	0.98	0.0069	0.99
Average	0.0048 ± 0.0007		0.0061 ± 0.0012	

The bottom row shows the mean and standard deviation of $d\chi_{\text{fat}}/dT$ over all samples

temperatures may have had an influence on the temperature dependence of the susceptibility. Dispersion of the lipid phase was observed in four of the fat tissue samples, and the effect seemed correlated with a lower abundance of residual water. Moreover, unsaturated lipids in human fat, e.g., containing oleic acid 18:1 (cis-9) alkyl chains, have much lower melting points than saturated lipids (containing palmitic acid 16:0) [11], resulting in a liquid fraction containing mostly unsaturated triacylglycerides at the top of the sample that float on the more solid, saturated fat tissue when held above 40°C for an extended amount of time. This may have added to the hysteresis effects observed for the susceptibility.

A spread in the χ values at starting temperature was also observed. The fat tissue samples were kept untreated to exclude pollution and verify that the original lipid components were preserved. For the same reason, we did not homogenize the samples prior to the measurements. However, the samples were surgically removed directly post-mortem, which led to the presence of blood traces in the fat. Even though the amount of blood was minimal, it varied over the samples and may have contributed to the range of found χ_{fat} values. It may also be explained by the experimental setup. The experimental setup employed a capillary-sphere plug-in. This specific shape complicates shimming of the sample. It was observed that the shim settings influenced the peak position of the sphere, $\delta_{\text{ref, sphere}}$, more than they influenced the capillary peak. A change in the peak position difference will influence the outcome for χ_{fat} (Eq. 5). The shimming process was therefore optimized per sample by minimizing the peak widths of $\delta_{\text{ref, sphere}}$ and $\delta_{\text{ref, capillary}}$. However, this effect still may have contributed to the observed spread in absolute χ_{fat} values.

Conclusion

In this work, the temperature dependence of the magnetic susceptibility of human breast fat was measured. The experiment was performed for six breast fat samples, all of which exhibited a linear temperature dependence of the susceptibility.

The average $d\chi_{\text{fat}}/dT$ values during temperature rise and temperature fall were 0.0048 ± 0.0007 ppm/°C and 0.0061 ± 0.0012 ppm/°C, respectively. In a previous work, heating experiments were conducted which showed that a temperature dependence of the susceptibility of ~ 0.005 ppm/°C leads to errors in MR temperature measurements [4]. The current work shows that human breast fat experiences heating-induced susceptibility changes. It is concluded that the impact of heat-induced susceptibility changes during thermal therapy of fatty tissues may not be neglected.

Open Access This article is distributed under the terms of the Creative Commons Attribution Noncommercial License which permits any noncommercial use, distribution, and reproduction in any medium, provided the original author(s) and source are credited.

References

- Hindman JC (1966) Proton resonance shift of water in the gas and liquid states. *J Chem Phys* 44:4582–4592
- Stollberger R, Ascher PW, Huber D, Renhart W, Radner H, Ebner F (1998) Temperature monitoring of interstitial thermal tissue coagulation using MR phase images 2. *J Magn Reson Imaging* 8(1):188–196
- De Poorter J (1995) Noninvasive MRI thermometry with the proton resonance frequency method: study of susceptibility effects. *Magn Reson Med* 34(3):359–367
- Sprinkhuizen SM, Konings MK, van der Bom MJ, Viergever MA, Bakker CJ, Bartels LW (2010) Temperature-induced tissue susceptibility changes lead to significant temperature errors in PRFS-based MR thermometry during thermal interventions. *Magn Reson Med* 64(5):1360–1372
- Young IR, Hajnal JV, Roberts IG, Ling JX, Hill-Cottingham RJ, Oatridge A, Wilson JA (1996) An evaluation of the effects of susceptibility changes on the water chemical shift method of temperature measurement in human peripheral muscle. *Magn Reson Med* 36(3):366–374
- Young IR, Bell JD, Hajnal JV, Jenkinson G, Ling J (1998) Evaluation of the stability of the proton chemical shifts of some metabolites other than water during thermal cycling of normal human muscle tissue. *J Magn Reson Imaging* 8(5):1114–1118
- Frei K, Bernstein HJ (1962) Method for determining magnetic susceptibilities by NMR. *J Chem Phys* 37:1891–1892

8. Hoffman RE, Becker ED (2005) Temperature dependence of the ^1H chemical shift of tetramethylsilane in chloroform, methanol, and dimethylsulfoxide. *J Magn Reson* 176(1):87–98
9. Ren J, Dimitrov I, Sherry AD, Malloy CR (2008) Composition of adipose tissue and marrow fat in humans by ^1H NMR at 7 Tesla. *J Lipid Res* 49(9):2055–2062
10. Hopkins JA, Wehrli FW (1997) Magnetic susceptibility measurement of insoluble solids by NMR: magnetic susceptibility of bone. *Magn Reson Med* 37(4):494–500
11. Cevc G (1991) How membrane chain-melting phase-transition temperature is affected by the lipid chain asymmetry and degree of unsaturation: an effective chain-length model. *Biochemistry* 30(29):7186–7193